

Chemistry A European Journal

 **Chemistry
Europe**
European Chemical
Societies Publishing

Accepted Article

Title: Revisiting Alkane Hydroxylation with *m*-CPBA
(*m*Chloroperbenzoic Acid) Catalyzed by Nickel(II) Complexes

Authors: Shinobu Itoh, Tomoya Shinke, Mayu Itoh, Takuma Wada,
Yuma Morimoto, Sachiko Yanagisawa, Hideki Sugimoto, and
Minoru Kubo

This manuscript has been accepted after peer review and appears as an Accepted Article online prior to editing, proofing, and formal publication of the final Version of Record (VoR). This work is currently citable by using the Digital Object Identifier (DOI) given below. The VoR will be published online in Early View as soon as possible and may be different to this Accepted Article as a result of editing. Readers should obtain the VoR from the journal website shown below when it is published to ensure accuracy of information. The authors are responsible for the content of this Accepted Article.

To be cited as: *Chem. Eur. J.* 10.1002/chem.202102532

Link to VoR: <https://doi.org/10.1002/chem.202102532>

WILEY-VCH

Revisiting Alkane Hydroxylation with *m*-CPBA (*m*-Chloroperbenzoic Acid) Catalyzed by Nickel(II) Complexes

Tomoya Shinke,^[a] Mayu Itoh,^[a] Takuma Wada,^[a] Yuma Morimoto,^[a] Sachiko Yanagisawa,^[b] Hideki Sugimoto,^[a] Minoru Kubo,^[b] and Shinobu Itoh*^[a]

[a] T. Shinke, M. Itoh, T. Wada, Assist. Prof. Y. Morimoto, Assoc. Prof. H. Sugimoto, Prof. S. Itoh
Department of Molecular Chemistry, Division of Applied Chemistry
Graduate School of Engineering, Osaka University
2-1 Yamadaoka, Suita, Osaka 565-0871, Japan
E-mail: shinobu@chem.eng.osaka-u.ac.jp
Twitter: @Shinoums

[b] Assoc. Prof. S. Yanagisawa, Prof. M. Kubo
Graduate School of Science, University of Hyogo
3-2-1 Koto, Kamigori-cho, Ako-gun, Hyogo 678-1297, Japan

Supporting information for this article is given via a link at the end of the document.

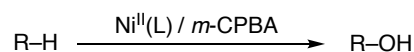
Abstract: Mechanistic studies are performed on the alkane hydroxylation with *m*-CPBA (*m*-chloroperbenzoic acid) catalyzed by nickel(II) complexes, Ni^{II}(L). In the oxidation of cycloalkanes, Ni^{II}(TPA) acts as an efficient catalyst with a high yield and a high alcohol selectivity. In the oxidation of adamantane, the tertiary carbon is predominantly oxidized. The reaction rate shows first-order dependence on [substrate] and [Ni^{II}(L)] but is independent on [*m*-CPBA]; $v_{\text{obs}} = k_2[\text{substrate}][\text{Ni}^{\text{II}}(\text{L})]$. The reaction exhibited a relatively large kinetic deuterium isotope effect (*KIE*) of 6.7, demonstrating that the hydrogen atom abstraction is involved in the rate-limiting step of the catalytic cycle. Furthermore, Ni^{II}(L) supported by related tetradentate ligands exhibit apparently different catalytic activity, suggesting contribution of the Ni^{II}(L) in the catalytic cycle. Based on the kinetic analysis and the significant effects of O₂ and CCl₄ on the product distribution pattern, possible contributions of (L)Ni^{II}-O• and the acyloxyl radical as the reactive oxidants are discussed.

Introduction

Alkanes are the most abundant chemicals obtained from crude oil and natural gas. In the present chemical industry and synthetic organic chemistry, selective hydroxylation of alkanes (saturated hydrocarbons) is an important chemical process to obtain valuable compounds such as alcohols, which themselves are also important precursors for the synthesis of various organic compounds.^[1] Thus, the selective alkane hydroxylation has long been one of the most important research objectives in catalytic chemistry.^[2] In nature, metalloenzymes such as cytochrome P450 and methane monooxygenases (MMOs) catalyze the hydroxylation of alkanes having strong C–H bonds (BDE ~100 kcal/mol) using molecular oxygen (O₂) as an oxidant with great efficiency and high alcohol-product selectivity under very mild conditions.^[3] Such metalloenzymes contain iron or copper at their active sites, and for that reason, a large number of iron- and copper-active-oxygen (superoxide, peroxide, oxyl radical, and oxide) intermediates have been studied extensively in model systems.^[4] More recently, iron- and copper-loaded zeolites have been demonstrated to be efficient catalysts for selective oxidation of methane to methanol, in which similar types of iron- and copper-

active-oxygen species have been invoked as the key reactive intermediates based on the spectroscopic and DFT studies.^[5]

In contrast to the large number of iron- and copper-active-oxygen complexes reported over the past decades, relatively few examples of such active-oxygen complexes of nickel have been explored.^[6] Nonetheless, Schwarz and co-workers demonstrated that NiO⁺ is an efficient oxidant for methane hydroxylation compared to FeO⁺ and MnO⁺ in the gas phase reaction,^[7] which is afterwards supported by theoretical calculations by Yoshizawa and co-workers.^[8] In this respect, we have demonstrated that nickel(II)-complexes, Ni^{II}(L), supported by tripodal N₄ ligands such as tris(2-pyridylmethyl)amine (TPA) and its analogues can catalyze oxygenation of alkanes by *m*-chloroperbenzoic acid (*m*-CPBA) in solution, where the yield of alcohol product and its selectivity (alcohol/ketone, *A/K*) are much better than those of the Fe- and Mn-complexes supported by the same ligand (TPA) (Scheme 1).^[9] Afterwards, we and other groups investigated the catalytic alkane hydroxylation reaction by *m*-CPBA using a variety of nickel(II) complexes to examine the ligand effects on the catalytic activity.^[10] Regarding to the reactive intermediate involved in the catalytic reaction, (L)Ni–O• (oxyl) species have been postulated based on the product analysis.^[10a]

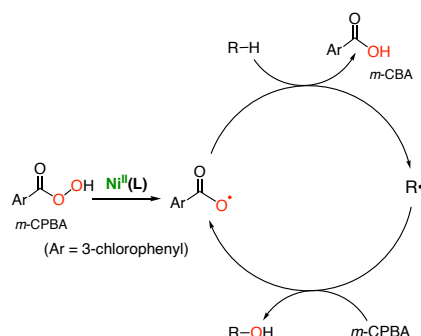


Scheme 1. Alkane hydroxylation with *m*-CPBA catalyzed by nickel(II)-complexes.

Meanwhile, Hartwig and co-worker conducted detailed mechanistic studies on the Ni^{II}(L)-catalyzed alkane oxidation reaction by *m*-CPBA to propose a free-radical chain mechanism shown in Scheme 2.^[11] In this mechanism, the reaction of *m*-CPBA and Ni^{II}(L) generates ArC(O)O• (aryloxyl radical, Ar = 3-chlorophenyl) as an active oxidant for the hydrogen atom abstraction (HAA) from the alkane substrates (R–H) giving *m*-CBA (*m*-chlorobenzoic acid) and radical intermediate of the substrate (R•). Then, the generated substrate radical R• reacts with another *m*-CPBA molecule to give the alcohol product R–OH and ArC(O)O•, making the catalytic cycle. In this mechanism, Ni^{II}(L) is considered as an initiator of the radical chain reaction to generate

FULL PAPER

ArC(O)O• from *m*-CPBA, but does not directly participate to the C–H bond activation process of R–H. However, little was discussed how ArC(O)O• was generated from the reaction of *m*-CPBA and Ni^{II}(L), and fate of the nickel complex afterwards.



Scheme 2. Hartwig's mechanism.

In this study, we revisited our alkane hydroxylation by *m*-CPBA with Ni^{II}-complexes supported by TPA and related tripodal tetradentate ligands to get deeper insights into the catalytic mechanism.

Results and Discussion

Alkane Hydroxylation with *m*-CPBA Catalyzed by Ni^{II}(TPA)

We have previously reported an efficient alkane hydroxylation by *m*-CPBA catalyzed by nickel(II) complex of TPA, [Ni^{II}(TPA)(OAc)(H₂O)](OAc) (Ni^{II}(TPA)) (Figure 1).^[9] Here, we re-examined the oxidation of cycloalkanes (CyⁿH: Cy⁶H, cyclohexane; Cy⁷H, cycloheptane; Cy⁸H: cyclooctane) by *m*-CPBA in the presence of a catalytic amount of Ni^{II}(TPA) (Table 1).

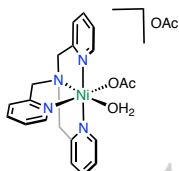


Figure 1. The structure of [Ni^{II}(TPA)(OAc)(H₂O)](OAc) (Ni^{II}(TPA)).

The reaction was started by adding *m*-CPBA (180 mM) to a CH₂Cl₂/CH₃CN (*v/v* = 3/1) solution containing a catalytic amount of Ni^{II}(TPA) (0.36 mM) and an excess amount of CyⁿH (2.2–2.7 M) at 30 °C under *anaerobic* conditions (N₂). After 2 h, the yields of alcohol (**A**), ketone (**K**), lactone (**L**), chlorocycloalkane (CyⁿCl) and chlorobenzene (PhCl, decarboxylation product of ArC(O)O•) were determined by GC-FID. As shown in Table 1, Ni^{II}(TPA) acted as an efficient catalyst to give **A** as the major product together with **K** as a minor product (entries 1–3). A small amount of **L** (ϵ -caprolactone), generated from **K** via Baeyer-Villiger reaction by *m*-CPBA, was also detected in the case of Cy⁶H (entry 1). However, the corresponding **L** was hardly detected in the cases of Cy⁷H and Cy⁸H (entries 2 and 3), since Baeyer-Villiger reaction of cyclohexanone was reported to be much faster than that of cycloheptanone and cyclooctanone.^[12] In this case, the alcohol product selectivity (**A**/(**K** + **L**)) increased as 5.8 → 8 → 18 as the bond dissociation energy of the C–H bond of the substrates decreases as 97.7 kcal/mol (Cy⁸H) → 96.5 kcal/mol (Cy⁷H) →

95.7 kcal/mol (Cy⁶H),^[13] indicating that the C–H bond activation of the substrates is involved in the alcohol formation process as discussed later based on the kinetic analysis. Notably, the product yield reached 95 % based on the oxidant (*m*-CPBA) in the case of Cy⁸H (entry 3), demonstrating that most of *m*-CPBA was used for the substrate oxidation. The chlorinated products (CyⁿCl) were also obtained, suggesting that cycloalkyl radical (Cyⁿ•) is generated by hydrogen atom abstraction from the substrate by the active oxidant. Generated Cyⁿ• may react with the solvent molecule (CH₂Cl₂) to give CyⁿCl. In fact, bromocyclohexane (Cy⁶Br) was obtained instead of Cy⁶Cl, when the reaction was carried out in CH₂Br₂/CH₃CN.

Table 1. Hydroxylation of cycloalkanes (CyⁿH) with *m*-CPBA catalyzed by Ni^{II}(TPA) under anaerobic condition (N₂) for 2 h.

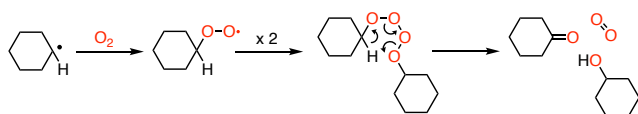
Cy ⁿ H	Yield (%) based on <i>m</i> -CPBA [a]						A/(K+L) ^[c]
	A	K	L	Cy ⁿ Cl	Total ^[b]	PhCl	
1 Cy ⁶ H	58	8.8	1.2	4.8	83	34	5.8
2 Cy ⁷ H	48	6.0	-	2.2	62	30	8
3 Cy ⁸ H	84	4.8	-	1.6	95	26	18
4 Cy ⁶ H ^[d]	9.0	3.6	9.2	1.4	36	1.2	0.70
5 Cy ⁶ H ^[d,e]	9.4	3.8	9.4	1.6	37	1.2	0.77

Reaction conditions: [Ni^{II}(TPA)] = 0.36 mM, [*m*-CPBA] = 0.18 M, [Cy⁶H] = 2.7 M, [Cy⁷H] = 2.4 M, [Cy⁸H] = 2.2 M in CH₂Cl₂/CH₃CN (*v/v* = 3/1) at 30 °C for 2 h under N₂. [a] The yields were determined by GC-FID using calibration curves of the products. [b] Total yield = **A** + 2**K** + 2**L** + CyⁿCl. [c] Alcohol product selectivity. [d] The reaction was carried out under O₂. [e] PPh₃ (2 equiv against *m*-CPBA) was added after the reaction.

Generation of Cyⁿ• (substrate radical) was also confirmed by the reaction carried out under O₂ atmosphere (Table 1, entry 4). In the *anaerobic* reaction of Cy⁶H (under N₂), **A** was obtained as the major product and the alcohol-product selectivity was quite high (entry 1). In this reaction, PhCl derived from *m*-CPBA was also generated in a relatively high yield (34 %). On the other hand, when the oxidation of Cy⁶H was carried out under O₂ atmosphere (entry 4), the product distribution pattern differed significantly from that of the *anaerobic* reaction under otherwise the same conditions. Namely, total yield of the oxidation products (**A** + **K** + **L** + Cy⁶Cl) as well as the yield of PhCl decreased significantly. Furthermore, the alcohol product selectivity **A**/(**K** + **L**) was completely lost. The result suggests that the radical intermediate is trapped by O₂ to induce "Russell rearrangement" (termination of radical chain reaction) (Scheme 3). Namely, generated cyclohexyl radical intermediate (Cy⁶•) via the hydrogen atom abstraction from Cy⁶H by a reactive oxidant rapidly reacts with O₂ at a rate of ~10⁹ M⁻¹ s⁻¹ to generate cyclohexyl peroxy radical species (Cy⁶OO•).^[14] Radical coupling between two Cy⁶OO• generates tetroxide Cy⁶OOOOOCy⁶, which is eventually converted to **A** and **K** in an equal amount.^[15] The reaction solution was analysed by GC-FID after addition of PPh₃ to get almost the same result to that of the aerobic reaction (entry 5). This result

FULL PAPER

suggested that $\text{Cy}^6\text{OO}\cdot$ was not converted to cyclohexyl hydrogen peroxide (Cy^6OOH) or cyclohexyl peroxide (Cy^6OOCy^6). If such peroxide products were formed in the aerobic reaction, **A** should be a major product after the treatment with PPh_3 .^[11]



Scheme 3. Russel rearrangement of tetroxide.

Hydroxylation of adamantane by *m*-CPBA also proceeded efficiently to give the corresponding alcohols, **3A** in 34 % and **2A** in 5 %, together with a small amount of ketone **2K** (2.6 %) (Prefixes 3 and 2 represent tertiary and secondary, respectively. The yields are calculated based on *m*-CPBA.) (Figure 2). As has been reported,^[9] the regioselectivity of the tertiary carbon (3°) against the secondary carbon (2°) was quite high ($3^\circ/2^\circ = 13$), suggesting that the reactive intermediate is not a highly reactive free radical species such as $\text{OH}\cdot$ as suggested by Hartwig *et al.*^[11, 16]

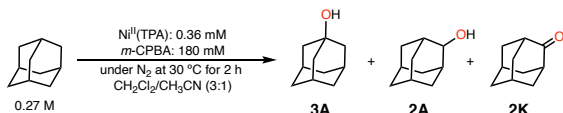


Figure 2. Hydroxylation of adamantane with *m*-CPBA catalyzed by $\text{Ni}^{\text{II}}(\text{TPA})$ in $\text{CH}_2\text{Cl}_2/\text{CH}_3\text{CN}$ ($v/v = 3/1$) under anaerobic conditions (N_2) for 2 h.

Kinetic Analysis

Kinetic analysis on the oxidation of Cy^6H was performed to get further insights into the catalytic mechanism. The reaction rates (v_{obs}) were obtained from the linear plots of the amounts of products (**A** + **K** + **L**, **M**) against the reaction time (s) at the initial stage (0 – 20 min) of the catalytic reaction using a lower concentration condition of the catalyst ($[\text{Ni}^{\text{II}}(\text{TPA})] = 0.036 - 0.18 \text{ mM}$). Figures S1(a), S1(b), and S1(c) show the plots obtained by changing the concentration of Cy^6H , $\text{Ni}^{\text{II}}(\text{TPA})$, and *m*-CPBA, respectively. In all cases, the product amounts increased linearly, from which the observed reaction rates (v_{obs} , M s^{-1}) were determined as the slopes. Then, the rate-dependences on the concentrations of Cy^6H , $\text{Ni}^{\text{II}}(\text{TPA})$, and *m*-CPBA were plotted as shown in Figure 3(a), 3(b), and 3(c), respectively. Apparently, the reaction rate (v_{obs}) exhibits first-order dependence on the concentrations of both Cy^6H and $\text{Ni}^{\text{II}}(\text{TPA})$ (Figures 3(a) and 3(b)) but was independent on the concentration of *m*-CPBA (Figure 3(c)) under the reaction conditions employed (see figure captions of Figure 3). Thus, the reaction rate can be expressed by eq (1), where k_2 was calculated as $0.22 \text{ M}^{-1} \text{ s}^{-1}$.

$$v_{\text{obs}} = k_2[\text{Cy}^6\text{H}][\text{Ni}^{\text{II}}(\text{TPA})] \quad (1)$$

The results indicate that *m*-CPBA itself is not involved in the turnover-limiting step (TLS) of the catalytic reaction. Thus, if the Hartwig mechanism (Scheme 2) operates, the reaction of $\text{R}\cdot$ and *m*-CPBA must be much faster than the reaction between $\text{ArC}(\text{O})\text{O}\cdot$ and $\text{R}-\text{H}$ giving *m*-CBA and $\text{R}\cdot$.

Catalytic hydroxylation of Cy^6D (C_6D_{12}) was also examined under the same reaction conditions to obtain the second-order rate constant k_2 as $3.3 \times 10^{-2} \text{ M}^{-1} \text{ s}^{-1}$ (Figure S2). Thus, the kinetic deuterium isotope effect, $k_2(\text{Cy}^6\text{H})/k_2(\text{Cy}^6\text{D})$, was obtained as 6.7,

clearly indicating that the hydrogen atom abstraction (HAA) is involve in the rate-limiting step of the catalytic cycle.

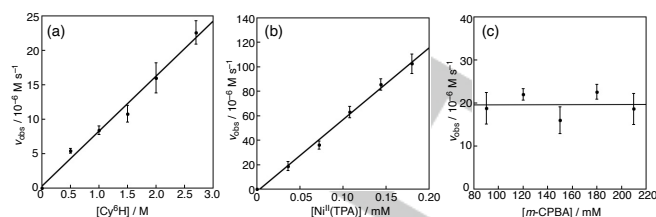


Figure 3. Kinetic analysis on the catalytic hydroxylation of cyclohexane (Cy^6H) with *m*-CPBA in the presence of a catalytic amount of $\text{Ni}^{\text{II}}(\text{TPA})$. (a) Plots of v_{obs} against the substrate concentration; $[\text{Cy}^6\text{H}] = 0.5-2.7 \text{ M}$, $[\text{m-CPBA}] = 180 \text{ mM}$, $[\text{Ni}^{\text{II}}(\text{TPA})] = 0.036 \text{ mM}$. (b) Plots of v_{obs} against the catalyst concentration; $[\text{Cy}^6\text{H}] = 2.7 \text{ M}$, $[\text{m-CPBA}] = 180 \text{ mM}$, $[\text{Ni}^{\text{II}}(\text{TPA})] = 0.036-0.18 \text{ mM}$. (c) Plots of v_{obs} against the oxidant concentration; $[\text{Cy}^6\text{H}] = 2.7 \text{ M}$, $[\text{m-CPBA}] = 80-220 \text{ mM}$, $[\text{Ni}^{\text{II}}(\text{TPA})] = 0.036 \text{ mM}$. (c). All reactions were conducted at least three times in $\text{CH}_2\text{Cl}_2/\text{CH}_3\text{CN}$ ($v/v = 3/1$) under N_2 at $30 \text{ }^\circ\text{C}$.

Catalytic Activity of Other Ni-complexes

In our previous study, we examined the catalytic activity of the Ni^{II} -complexes supported by a series of tetradentate ligands having one, two, or three 2,4-di-*tert*-butyl phenol group(s) (L1^{tBuH} , $\text{L2}^{\text{tBuH}_2}$, and $\text{L3}^{\text{tBuH}_3}$, Figure 4) in the oxidation of Cy^6H by *m*-CPBA.^[10a, 10b] To get further insights into the reaction mechanism, catalytic activities of these Ni^{II} -complexes were re-examined.

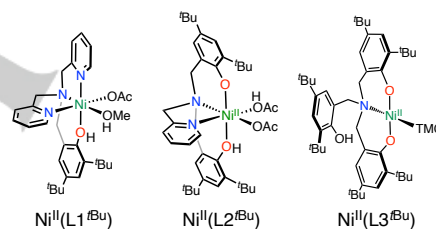


Figure 4. Ni^{II} -complexes supported by phenol(ate) ligands. TMG is 1,1,3,3-tetramethylguanidine. The syntheses and structural characterizations of these Ni^{II} -complexes were reported in our previous papers.^[10a, 10b]

In Figure 5 is shown the plots of product amounts against the reaction time for each complex in the oxidation of Cy^6H , and the amounts of products obtained after 15 min and the observed reaction rates (v_{obs} , M s^{-1}) are summarized in Table S1. In these cases as well, **A** was obtained as the major product together with **K**, **L**, and Cy^6Cl as the minor products. Apparently, reactivity of the four complexes was different ($v_{\text{obs}} = 23 \times 10^{-6} \text{ M s}^{-1}$ for $\text{Ni}^{\text{II}}(\text{TPA})$; $32 \times 10^{-6} \text{ M s}^{-1}$ for $\text{Ni}^{\text{II}}(\text{L1}^{\text{tBu}})$; $14 \times 10^{-6} \text{ M s}^{-1}$ for $\text{Ni}^{\text{II}}(\text{L2}^{\text{tBu}})$; $6.0 \times 10^{-6} \text{ M s}^{-1}$ for $\text{Ni}^{\text{II}}(\text{L3}^{\text{tBu}})$) and the monophenol

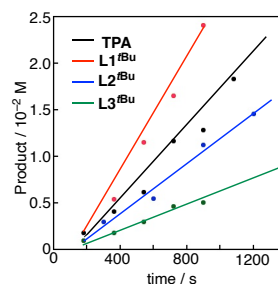


Figure 5. Plots of the product amounts against the reaction time in the catalytic hydroxylation of Cy^6H (2.7 M) with *m*-CPBA (180 mM) catalyzed by Ni^{II} -complexes (0.036 mM) in $\text{CH}_2\text{Cl}_2/\text{CH}_3\text{CN}$ ($v/v = 3/1$) under N_2 at room temperature. ($30 \text{ }^\circ\text{C}$).

FULL PAPER

complex $\text{Ni}^{\text{II}}(\text{L}^{\text{Ibu}})$ exhibited the highest catalytic activity (Table S1). The result indicates that an active oxidant derived from $\text{Ni}^{\text{II}}(\text{L})$ contributes to the catalytic reaction, as suggested by the kinetic result shown in Figure 3(b).

Reactive Oxidants for HAA

1. Aroyloxy Radical ($\text{ArC}(\text{O})\text{O}\cdot$)

As mentioned in Introduction, Hartwig and co-worker proposed a catalytic mechanism, in which the reaction of *m*-CPBA and $\text{Ni}^{\text{II}}(\text{L})$ generates aroyloxy radical ($\text{ArC}(\text{O})\text{O}\cdot$) as an active oxidant for HAA from R–H, generating the radical intermediate of the substrate ($\text{R}\cdot$) (Scheme 2).^[11] Then, the hydroxylation takes place by the reaction of generated $\text{R}\cdot$ and another molecule of *m*-CPBA, giving the alcohol product (R–OH) and re-generating $\text{ArC}(\text{O})\text{O}\cdot$, constructing a radical chain cycle. An essentially the same mechanism was proposed for the self-decomposition of peroxybenzoic acid in hydrocarbons.^[17] Thus, in the Hartwig's mechanism, $\text{Ni}^{\text{II}}(\text{L})$ is just an initiator of the radical chain reaction to generate $\text{ArC}(\text{O})\text{O}\cdot$. The observed different reactivities among the nickel(II) complexes examined in their study were attributed to the different rate of decomposition of *m*-CPBA to $\text{ArC}(\text{O})\text{O}\cdot$. However, the fate of $\text{Ni}^{\text{II}}(\text{L})$ after the reaction with *m*-CPBA was not discussed in the Hartwig's system.^[11] The reaction between $\text{Ni}^{\text{II}}(\text{L})$ and *m*-CPBA may generate an *m*-CPBA adduct of $\text{Ni}^{\text{II}}(\text{L})$, $(\text{L})\text{Ni}^{\text{II}}\text{-OOC}(\text{O})\text{Ar}$ (**a**).^[18] Then, O–O homolysis takes place to generate $\text{ArC}(\text{O})\text{O}\cdot$ and $(\text{L})\text{Ni}^{\text{II}}\text{-O}\cdot$. Generate $\text{ArC}(\text{O})\text{O}\cdot$ can be a reactive oxidant as proposed in the Hartwig mechanism (Scheme 2), since $\text{ArC}(\text{O})\text{O}\cdot$ is a powerful oxidant, judging from the high $\text{BDE}_{\text{O-H}}$ of $\text{ArC}(\text{O})\text{OH}$ (107.3 kcal/mol).^[13]

2. Nickel(II)-oxyl ($(\text{L})\text{Ni}^{\text{II}}\text{-O}\cdot$)

What about the reactivity of $(\text{L})\text{Ni}^{\text{II}}\text{-O}\cdot$ generated by the O–O bond homolysis of the *m*-CPBA adduct **a**? So far, little is known about the HAA reactivity of $(\text{L})\text{Ni}^{\text{II}}\text{-O}\cdot$ species, since there has been no report of $\text{BDE}_{\text{O-H}}$ of $(\text{L})\text{Ni}^{\text{II}}\text{-OH}$. Ray and coworkers reported that the reaction of a $\text{Ni}^{\text{II}}(\text{L})$ supported by a strongly electron donating tripodal tetradentate ligand TMG₃tren (L: tris[2-(*N*-tetramethylguanidyl)ethyl] amine) and *m*-CPBA generated a nickel terminal oxygen intermediate with $S = 1/2$, which could be formed via O–O bond homolysis of an *m*-CPBA adduct complex.^[19] This intermediate induced aliphatic ligand hydroxylation at the methyl group of the TMG (tetramethylguanidyl) substituent even at $-30\text{ }^{\circ}\text{C}$ ($\text{BDE}_{\text{C-H}}$ of N-CH_3 is about 93 kcal/mol).^[13]

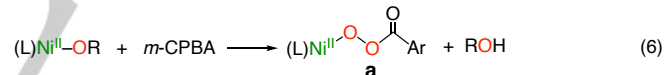
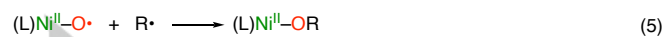
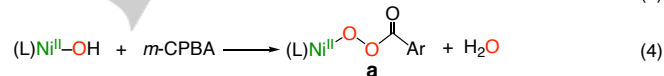
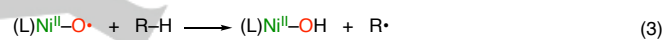
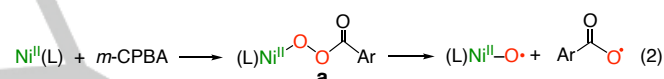
Company *et al.* and McDonald *et al.* independently investigated the reaction of $\text{Ni}^{\text{II}}(\text{L})$ supported by 2,6-diamidopyridine ligands with *m*-CPBA at low temperature to obtain $\text{Ni}^{\text{II}}\text{-O}\cdot$ type intermediates, which could be generated via O–O bond heterolysis of the *m*-CPBA adduct.^[20] In these reactions, however, they used strongly electron-donating dianionic diamido ligands (L^{2-}), so that the reactivity of the generated $\text{Ni}^{\text{II}}\text{-m-CPBA}$ adducts might be significantly different from those of the $\text{Ni}^{\text{II}}\text{-m-CPBA}$ adducts supported by the neutral nitrogen ligands.

On the other hand, Oda and co-workers succeeded to generate and characterize a distinct $\text{Zn}^{\text{II}}\text{-O}\cdot$ species in a zeolite super cage. They also reported that the generated $\text{Zn}^{\text{II}}\text{-O}\cdot$ species can oxidize methane ($\text{BDE}_{\text{C-H}} = 105\text{ kcal/mol}$) to methanol, demonstrating extremely high HAA reactivity of the oxyl-complex of late-transition metal ions.^[21] Moreover, Schwarz and co-

workers demonstrated that NiO^+ (formally $[\text{Ni}^{\text{II}}\text{-O}\cdot]^+$) is an efficient oxidant for methane hydroxylation in the gas phase reaction.^[7]

Judging from those reports, we propose that not only the aroyloxy radical ($\text{ArC}(\text{O})\text{O}\cdot$) but also $(\text{L})\text{Ni}^{\text{II}}\text{-O}\cdot$ species generated by the O–O homolysis of the nickel(II)-*m*-CPBA adduct **a** is a reactive oxidant in the catalytic alkane oxidation reaction (eq 2). Generated $\text{ArC}(\text{O})\text{O}\cdot$ in eq 2 can get into the catalytic cycle of the Hartwig's mechanism (Scheme 2). On the other hand, $(\text{L})\text{Ni}^{\text{II}}\text{-O}\cdot$ may also abstract hydrogen atom from R–H to generate $(\text{L})\text{Ni}^{\text{II}}\text{-OH}$ and $\text{R}\cdot$ (eq 3). Then, $(\text{L})\text{Ni}^{\text{II}}\text{-OH}$ undergoes ligand exchange reaction with another *m*-CPBA molecule to regenerate the *m*-CPBA adduct complex **a** and H_2O (eq 4). The substrate radical $\text{R}\cdot$ can also go into the catalytic cycle of Hartwig's mechanism (Scheme 2) and/or rebound to $(\text{L})\text{Ni}^{\text{II}}\text{-O}\cdot$ to produce $(\text{L})\text{Ni}^{\text{II}}\text{-OR}$ (eq 5), which can also undergo ligand exchange reaction with *m*-CPBA to regenerate **a** and alcohol product ROH (eq 6).

The bond dissociation energy of the O–O bond in the *m*-CPBA adduct **a** is not known, but it might be less than 40 kcal/mol, judging from the $\text{BDE}_{\text{O-O}}$ of the simple alkyl peroxybenzoic acid ($\text{RC}(\text{O})\text{OOH}$).^[13] If so, the endergonic O–O bond homolytic cleavage is involved in the rate-limiting process, being consistent with our kinetic analysis (eq 1). Namely, independence of v_{obs} on $[\text{m-CPBA}]$ suggested that generation of $\text{Ni}^{\text{II}}(\text{L})$ derived oxidant, $(\text{L})\text{Ni}^{\text{II}}\text{-O}\cdot$, from the *m*-CPBA adduct **a** is slower than the formation of **a** from $\text{Ni}^{\text{II}}(\text{L})$ and *m*-CPBA (eqs 1 and 2).



Involvement of $(\text{L})\text{Ni}^{\text{II}}\text{-O}\cdot$ in the HAA process can be evaluated by the following experiment (Figure 6). When the catalytic oxidation of Cy^6H (2.7 M) by *m*-CPBA (180 mM) was carried out in the presence of a catalytic amount of $\text{Ni}^{\text{II}}(\text{TPA})$ (0.36 mM) using a $\text{CCl}_4/\text{CH}_3\text{CN}$ ($v/v = 3/1$) mixed solvent instead of $\text{CH}_2\text{Cl}_2/\text{CH}_3\text{CN}$ ($v/v = 3/1$) for 6 h, chlorinated product Cy^6Cl was obtained as the major product (241 mM) together with **A** (4 mM), **K** (6 mM), and **L** (6 mM) as the minor products. At this point, all *m*-CPBA (180 mM) was consumed to provide *m*-CBA (175 mM) and PhCl (5 mM). Apparently, the product distribution pattern was largely different from that in the reaction carried out in $\text{CH}_2\text{Cl}_2/\text{CH}_3\text{CN}$ shown in Table 1. Since **L** was formed by Baeyer-Villiger oxidation of **K** with *m*-CPBA, 174 mM of *m*-CPBA (180 – 6 mM) can be used for the oxidation of Cy^6H . Notably, the total amount of the oxidation products was 257 mM (241 mM (Cy^6Cl) + 4 mM (**A**) + 6 mM (**K**) + 6 mM (**L**); Since both **K** and **L** are derived from **A**, the amounts of **K** and **L** are counted as the oxidation product from Cy^6H), which largely exceeded the amount of oxidant ($[\text{m-CPBA}] = 174\text{ mM}$). This means that different oxidants other than $\text{ArC}(\text{O})\text{O}\cdot$ and $\text{Ar}\cdot$ (decarboxylation product of $\text{ArC}(\text{O})\text{O}\cdot$, see below) are involved for the HAA process from the substrate. In other words, if all the oxidation products (**A**, **K**, **L**, and Cy^6Cl) were produced from $\text{Cy}^6\cdot$ intermediate, 257 mM of oxidants (hydrogen atom abstractor) are needed. Out of the 257 mM oxidant, 40 mM of $\text{CCl}_3\cdot$, generated

FULL PAPER

by the reaction of $\text{Cy}^6\cdot$ and CCl_4 , could be an oxidant, since 40 mM of CHCl_3 was obtained (Figure 6). Thus, at least 43 mM (257 – 40 – 174 mM) of nickel-based oxidant should be derived from the *m*-CPBA adduct **a**, that must be $(\text{L})\text{Ni}^{\text{II}}\text{-O}\cdot$. Namely, involvement of $(\text{L})\text{Ni}^{\text{II}}\text{-O}\cdot$ could not be neglected in the catalytic alkane oxidation reaction.

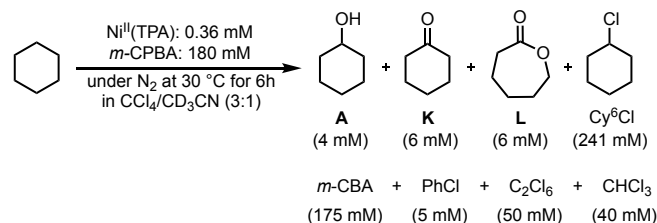


Figure 6. Oxidation of Cy^6H by *m*-CPBA with $\text{Ni}^{\text{II}}(\text{TPA})$ in $\text{CCl}_4/\text{CD}_3\text{CN}$ (3:1). The product yields shown in parentheses were determined by GC-FID and $^1\text{H-NMR}$.

3. 3-Chlorophenyl Radical ($\text{Ar}\cdot$)

As discussed in the Hartwig paper, the C–H bond activation of R–H by $\text{ArC}(\text{O})\text{O}\cdot$ may compete with decarboxylation from $\text{ArC}(\text{O})\text{O}\cdot$ ($<10^{4-5} \text{ s}^{-1}$)^[22] giving $\cdot\text{C}_6\text{H}_4\text{Cl}$ ($\text{Ar}\cdot$) and CO_2 . The generated $\text{Ar}\cdot$ can also abstract hydrogen atom from the substrate (R–H) or the solvent molecule to generate ArH (PhCl). To confirm this possibility, the following reactions were carried out. When the catalytic hydroxylation was carried out using Cy^6D (cyclohexane-*d*₁₂) instead of Cy^6H in $\text{CH}_2\text{Cl}_2/\text{CH}_3\text{CN}$, 30 % of PhCl was deuterated (determined by simulation of the mass spectra shown in Figure S3). In the reaction of Cy^6H in $\text{CD}_2\text{Cl}_2/\text{CD}_3\text{CN}$, PhCl was also deuterated in 6 %. These results confirmed that hydrogen (deuteron) atom abstraction by chlorobenzene radical ($\text{Ar}\cdot$) occurs both from the substrate and from the solvent.

Trapping of $(\text{L})\text{Ni}\text{-O}\cdot$ Species

To confirm the O–O bond cleavage occurring from the *m*-CPBA adduct **a**, a reaction of the Ni^{II} -complex of the diphenol ligand $\text{Ni}(\text{L}2^{\text{Bu}})$ and *m*-CPBA was examined at a low temperature. Figure 7(a) shows an absorption spectrum obtained upon addition of an equimolar amount of *m*-CPBA to an acetone solution of $\text{Ni}(\text{L}2^{\text{Bu}})$ in the presence of a base such as DBU (1,8-diazabicyclo[5.4.0]undec-7-ene, 2 equiv) at $-70 \text{ }^\circ\text{C}$, which exhibits a visible absorption band at 547 nm ($\epsilon = 1246 \text{ M}^{-1} \text{ cm}^{-1}$) together with a broad near-IR absorption band at 1280 nm ($\epsilon = 1105 \text{ M}^{-1} \text{ cm}^{-1}$). The broad absorption band in the near-IR region is reminiscent of a phenolate to phenoxyl-radical inter-valence charge transfer (IVCT) of one-electron oxidized transition-metal complexes of diphenolate ligands.^[23]

The resonance Raman spectrum of the generated intermediate, taken with 405 nm excitation at $-80 \text{ }^\circ\text{C}$, exhibited a Raman band at 1572 cm^{-1} , which disappeared by raising the temperature (Figure 7b). This band is assignable to ν_{8a} ($\text{C}_{\text{ortho}}\text{-C}_{\text{meta}}$ stretching vibration) of the phenoxyl-radical species. A weak band was also recognized at 1499 cm^{-1} , a frequency characteristic of ν_{7a} (C–O stretching vibration). These two band frequencies are relatively low, as compared to square-planar Ni-phenoxyl radical complexes with a variety of salen-type ligand systems ($1589\text{-}1612 \text{ cm}^{-1}$ for ν_{8a} and $1507\text{-}1517 \text{ cm}^{-1}$ for ν_{7a}).^[24] The frequencies of ν_{8a} and ν_{7a} for Ni-phenoxyl radical complexes are sensitive to the coordination structures, and tend to be downshifted by Ni–O bond elongation.^[25] Particularly, octahedral Ni^{II} -complexes ligated by a salen and two axial pyridines have weak Ni–O bonds, giving rather

low frequencies of ν_{8a} ($1582\text{-}1585 \text{ cm}^{-1}$) and ν_{7a} ($1494\text{-}1498 \text{ cm}^{-1}$).^[25b] Thus, the observed low frequencies of ν_{8a} and ν_{7a} for the Ni^{II} -complex intermediate could be derived from weak interaction between the phenoxyl-radical moiety and the nickel center in the octahedral coordination geometry.

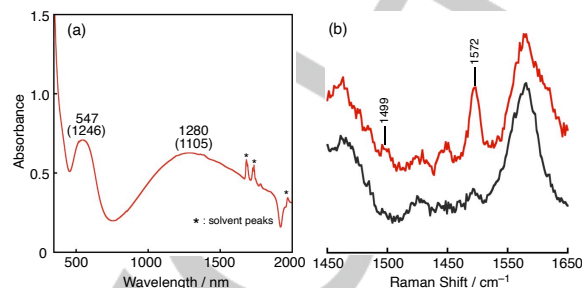


Figure 7. (a) UV-vis-NIR spectrum of generated intermediate by the reaction of $\text{Ni}(\text{L}2^{\text{Bu}})$ (0.57 mM) with *m*-CPBA (1 equiv) in the presence of DBU (2.5 equiv) in acetone at $-70 \text{ }^\circ\text{C}$. (b) Resonance Raman spectrum of the intermediate derived from the reaction of $\text{Ni}(\text{L}2^{\text{Bu}})$ with 2.5 equiv of DBU and 1 equiv of *m*-CPBA in acetone at $-80 \text{ }^\circ\text{C}$, excited by 405 nm laser light (red line), and that after decomposition by raising the temperature to room temperature (black line).

The electro-spray ionization mass spectroscopy (ESI-MS) with negative ion mode exhibited a peak cluster at m/z 675.34, even though the peak intensity was small due to its instability under the ESI-MS measurement. The peak positions as well as the isotope distribution pattern of which were consistent with the chemical formula of $[\text{Ni}(\text{L}2^{\text{Bu}})(\text{O})(\text{OAc})]^-$ (Figure 8). The $^1\text{H-NMR}$ spectrum of the final reaction solution showed existence of *m*-CBA (*m*-chlorobenzoic acid) as a decomposition product of *m*-CPBA in an 83 % yield.

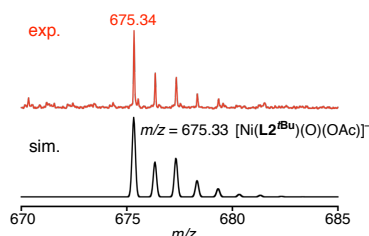
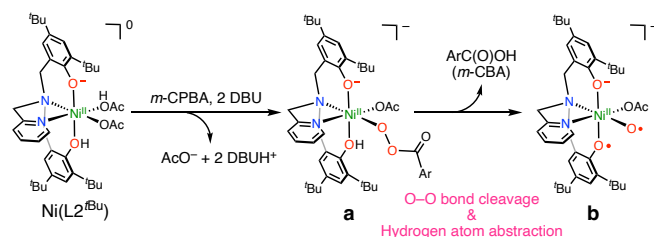


Figure 8. Negative mode ESI-MS of the intermediate (red line) generated by the reaction of $\text{Ni}(\text{L}2^{\text{Bu}})$ (1.0 mM) and *m*-CPBA (1 equiv) in the presence of DBU (2 eq) in acetone at $-70 \text{ }^\circ\text{C}$ and its simulation spectrum (black line).

These results (UV-vis-NIR, resonance Raman, and ESI-MS) can be explained by assuming a reaction mechanism shown in Scheme 4. The reaction of the neutral nickel(II) complex of the diphenol ligand, $\text{Ni}(\text{L}2^{\text{Bu}})$ ($[\text{Ni}^{\text{II}}(\text{L}2^{\text{Bu}}\text{H}^-)(\text{AcO}^-)(\text{AcOH})]$), with 1 equiv of *m*-CPBA in the presence of 2 equiv of DBU generates a monoanionic *m*-CPBA adduct **a** by releasing 1 equiv of AcO^- and 2 equiv of protonated DBU (DBUH^+). Then, homolytic cleavage of the O–O bond occurs concomitant with intramolecular hydrogen atom abstraction (HAA) from the remained phenol group in **a** by dissociated $\text{ArC}(\text{O})\text{O}\cdot$, generating a monoanionic $\text{Ni}^{\text{II}}\text{-O}\cdot$ species **b** supported by a phenoxyl-radical/phenolate ligand, $[\text{Ni}^{\text{II}}(\text{L}2^{\text{Bu}}\cdot)(\text{O}\cdot)(\text{AcO}^-)]^-$, and *m*-CBA. Although further studies are needed to evaluate detailed structure of **b**, the results suggest that the O–O bond homolytic cleavage occurs in the nickel(II)-*m*-CPBA adduct intermediate **a** to generate the $\text{Ni}^{\text{II}}\text{-O}\cdot$ species and $\text{ArC}(\text{O})\text{O}\cdot$, the later of which abstracts hydrogen atom

FULL PAPER

from the phenol moiety of the supporting ligand. Thus, this reaction can be regarded as a model reaction of the HAA process of the catalytic cycle.



Scheme 4. Reaction of Ni(L2^{tBu}) and *m*-CPBA generating Ni^{II}-O• species.

Conclusion

In this study, catalytic hydroxylation reactions of alkanes with *m*-CPBA catalyzed by Ni^{II}(TPA) and related Ni^{II}-complexes were reinvestigated. Most of the results obtained in this study are consistent with the Hartwig's mechanism shown in Scheme 2, where the aryloxy radical ArC(O)O• generated via O–O bond homolysis of *m*-CPBA itself is a reactive oxidant for HAA from the alkane substrate. However, our present results suggested that (L)Ni^{II}-O• generated by the O–O bond homolysis of the (L)Ni^{II}-*m*-CPBA adduct **a** can also contribute to the HAA process in the alkane hydroxylation reaction.

Experimental Section

General

The reagents and the solvents used in this study, except the ligands and the nickel(II) complexes, were commercial products of the highest available purity and further purified by the standard methods, if necessary.^[26] *m*-Chloroperbenzoic acid (*m*-CPBA) was washed using 0.07 M phosphate buffer (pH = 8.5) and recrystallized from dichloromethane before use. Ligands, TPA, ^tBu₂L1H, ^tBu₂L2H₂ and ^tBu₂L3H₃, and their nickel(II) complexes were prepared according to the reported procedures.^[9–10] Anaerobic reactions were carried out under N₂ atmosphere using a glovebox (miwa DB0-1KP or KK-01-AS, KOREA KIYON product, [O₂] < 1 ppm). UV-visible spectra were taken on a Jasco V-570 or a Hewlett Packard 8453 photo diode array spectrophotometer equipped with a Unisoku thermostated cryostat cell holder USP-203. Visible-to-NIR spectra were taken on Jasco V-670. ¹H-NMR spectra were recorded on a JEOL ECP400. ESI-MS (electrospray ionization mass spectra) measurements were performed on a BRUKER cryospray microTOFII. Resonance Raman scattering was excited at 405 nm with a diode laser (Ondax, SureLock Model LM-405-PLR-40-2). Resonance Raman scattering was dispersed by a 1-m single spectrometer (MG100DG; Ritsu Ohyo Kogaku) and was detected by a liquid nitrogen cooled CCD detector (Symphony; Horiba Jobin Yvon). The resonance Raman measurement was carried out using a spinning NMR tube at –80 °C by flashing cooled dinitrogen gas. Gas chromatography (flame ionization detector (GC-FID)) measurements were performed on a Shimadzu GC-2010 equipped with a GL Science InertCapWAX capillary column (30 m × 0.25 mm), an AOC-20s auto sampler, and an AOC-20i auto injector.

Catalytic oxidation

All procedures of the catalytic hydroxylation reactions were carried out under inert atmospheres (N₂) unless otherwise noted. The reaction was started by adding *m*-CPBA to a solution containing the nickel complex and a substrate. The reaction conditions are shown in the footnotes of Tables. After quenching the reaction by passing the reaction mixture through a

short alumina-column, products were analysed by using GC-FID. All peaks of interest were identified by comparing the retention times with those of the authentic samples. The products were quantified by comparing their peak areas with that of an internal standard (nitrobenzene) using calibration curves consisting of plots of molar ratio (moles of organic compound/moles of internal standard) versus area ratio (area of organic compound/area of standard).

Acknowledgements

The present work was supported by CREST (JPMJCR16P1) from JST and by Grant-in-Aid for Challenging Research (Exploratory) (19K22201) from JSPS. The authors also thank Prof. Yumi Yakiyama and Prof. Hidehiro Sakurai of Osaka university for their assistance to obtain the near-IR spectra.

Keywords: Catalytic alkane hydroxylation • nickel(II) complex • Aryloxy radical • nickel oxyl • hydrogen atom abstraction

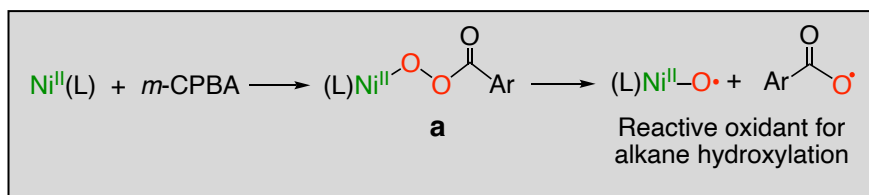
- [1] F. A. Carey, R. J. Sundberg, *Advanced Organic Chemistry, Part B: Reaction and Synthesis*, 5th ed., Springer-Verlag, New York, 2007.
- [2] J. Haggin, *Chem. Eng. News Arch.* **1993**, *71*, 23–27.
- [3] a) P. R. Ortiz de Montellano, *Chem. Rev.* **2010**, *110*, 932–948; b) M.-H. Baik, M. Newcomb, R. A. Friesner, S. J. Lippard, *Chem. Rev.* **2003**, *103*, 2385–2420; c) M. O. Ross, A. C. Rosenzweig, *J. Biol. Inorg. Chem.* **2017**, *22*, 307–319; d) V. C. C. Wang, S. Maji, P. P. Y. Chen, H. K. Lee, S. S. F. Yu, S. I. Chan, *Chem. Rev.* **2017**, *117*, 8574–8621.
- [4] a) M. Momenteau, C. A. Reed, *Chem. Rev.* **1994**, *94*, 659–698; b) L. Que, R. Y. N. Ho, *Chem. Rev.* **1996**, *96*, 2607–2624; c) M. Costas, M. P. Mehn, M. P. Jensen, L. Que, *Chem. Rev.* **2004**, *104*, 939–986; d) T. J. Collins, A. D. Ryabov, *Chem. Rev.* **2017**, *117*, 9140–9162; e) X. Huang, J. T. Groves, *J. Biol. Inorg. Chem.* **2017**, *22*, 185–207; f) G. Olivo, O. Cussó, M. Borrell, M. Costas, *J. Biol. Inorg. Chem.* **2017**, *22*, 425–452; g) S. Sahu, D. P. Goldberg, *J. Am. Chem. Soc.* **2016**, *138*, 11410–11428; h) M. Guo, T. Corona, K. Ray, W. Nam, *ACS Cent. Sci.* **2019**, *5*, 13–28; i) E. A. Lewis, W. B. Tolman, *Chem. Rev.* **2004**, *104*, 1047–1076; j) L. M. Mirica, X. Ottenwaelder, T. D. P. Stack, *Chem. Rev.* **2004**, *104*, 1013–1045; k) E. I. Solomon, D. E. Heppner, E. M. Johnston, J. W. Ginsbach, J. Cirera, M. Qayyum, M. T. Kieber-Emmons, C. H. Kjaergaard, R. G. Hadt, L. Tian, *Chem. Rev.* **2014**, *114*, 3659–3853; l) C. E. Elwell, N. L. Gagnon, B. D. Neisen, D. Dhar, A. D. Spaeth, G. M. Yee, W. B. Tolman, *Chem. Rev.* **2017**, *117*, 2059–2107; m) D. A. Quist, D. E. Diaz, J. J. Liu, K. D. Karlin, *J. Biol. Inorg. Chem.* **2017**, *22*, 253–288.
- [5] a) P. Schwach, X. Pan, X. Bao, *Chem. Rev.* **2017**, *117*, 8497–8520; b) B. E. R. Snyder, M. L. Bols, R. A. Schoonheydt, B. F. Sels, E. I. Solomon, *Chem. Rev.* **2018**, *118*, 2718–2768; c) M. H. Mahyuddin, Y. Shiota, K. Yoshizawa, *Catal. Sci. Technol.* **2019**, *9*, 1744–1768; d) M. A. Newton, A. J. Knorpp, V. L. Sushkevich, D. Palagin, J. A. van Bokhoven, *Chem. Soc. Rev.* **2020**, *49*, 1449–1486.
- [6] a) S. Hikichi, M. Akita, Y. Moro-oka, *Coord. Chem. Rev.* **2000**, *198*, 61–87; b) K. Ray, F. Heims, F. F. Pfaff, *Eur. J. Inorg. Chem.* **2013**, *2013*, 3784–3807; c) T. Corona, A. Company, *Chem.–Eur. J.* **2016**, *22*, 13422–13429; d) A. T. Fiedler, A. A. Fischer, *J. Biol. Inorg. Chem.* **2017**, *22*, 407–424; e) C.-Y. Lin, P. P. Power, *Chem. Soc. Rev.* **2017**, *46*, 5347–5399; f) P. Pirovano, A. R. McDonald, *Eur. J. Inorg. Chem.* **2018**, *2018*, 547–560.
- [7] D. Schröder, H. Schwarz, *Angew. Chem., Int. Ed. Engl.* **1995**, *34*, 1973–1995; *Angew. Chem.* **1995**, *107*, 2126–2150.
- [8] Y. Shiota, K. Yoshizawa, *J. Am. Chem. Soc.* **2000**, *122*, 12317–12326.
- [9] T. Nagataki, Y. Tachi, S. Itoh, *Chem. Commun.* **2006**, 4016–4018.
- [10] a) T. Nagataki, K. Ishii, Y. Tachi, S. Itoh, *Dalton Trans.* **2007**, 1120–1128; b) T. Nagataki, S. Itoh, *Chem. Lett.* **2007**, *36*, 748–749; c) M. Balamurugan, R. Mayilmurugan, E. Suresh, M. Palaniandavar, *Dalton Trans.* **2011**, *40*, 9413–9424; d) M. Sankaralingam, P. Vadivelu, E. Suresh, M. Palaniandavar, *Inorg. Chim. Acta* **2013**, *407*, 98–107; e) S. Hikichi, K. Hanaue, T. Fujimura, H. Okuda, J. Nakazawa, Y. Ohzu, C.

FULL PAPER

- Kobayashi, M. Akita, *Dalton Trans.* **2013**, 42, 3346-3356; f) J. Nakazawa, S. Terada, M. Yamada, S. Hikichi, *J. Am. Chem. Soc.* **2013**, 135, 6010-6013; g) M. Sankaralingam, M. Balamurugan, M. Palaniandavar, P. Vadivelu, C. H. Suresh, *Chem. Eur. J.* **2014**, 20, 11346-11361; h) D. D. Narulkar, A. R. Patil, C. C. Naik, S. N. Dhuri, *Inorg. Chim. Acta* **2015**, 427, 248-258; i) M. Sankaralingam, P. Vadivelu, M. Palaniandavar, *Dalton Trans.* **2017**, 46, 7181-7193; j) M. Sankaralingam, M. Balamurugan, M. Palaniandavar, *Coord. Chem. Rev.* **2020**, 403, 213085.
- [11] Y. Qiu, J. F. Hartwig, *J. Am. Chem. Soc.* **2020**, 142, 19239-19248.
- [12] a) S. L. Friess, P. E. Frankenburg, *J. Am. Chem. Soc.* **1952**, 74, 2679-2680; b) P. S. Starcher, B. Phillips, *J. Am. Chem. Soc.* **1958**, 80, 4079-4082; c) Y.-D. Wu, K. N. Houk, M. N. Paddon-Row, *Angew. Chem., Int. Ed. Engl.* **1992**, 31, 1019-1021; *Angew. Chem.* **1992**, 104, 1087-1089.
- [13] Y.-R. Luo, *Comprehensive Handbook of Chemical Bond Energy*, CRC Press, Boca Raton, London, New York, **2007**.
- [14] B. Maillard, K. U. Ingold, J. C. Scaiano, *J. Am. Chem. Soc.* **1983**, 105, 5095-5099.
- [15] K. U. Ingold, *Can. J. Chem.* **1969**, 47, 3803-3808.
- [16] D. T. Sawyer, A. Sobkowiak, T. Matsushita, *Acc. Chem. Res.* **1996**, 29, 409-416.
- [17] T. Katsumi, S. Osamu, *Bull. Chem. Soc. Jpn.* **1962**, 35, 1678-1683.
- [18] S. Hikichi, C. Kobayashi, M. Yoshizawa, M. Akita, *Chem. Asian J.* **2010**, 5, 2086-2092.
- [19] F. F. Pfaff, F. Heims, S. Kundu, S. Mebs, K. Ray, *Chem. Commun.* **2012**, 48, 3730-3732.
- [20] a) T. Corona, F. F. Pfaff, F. Acuña-Parés, A. Draksharapu, C. J. Whiteoak, V. Martin-Diaconescu, J. Lloret-Fillol, W. R. Browne, K. Ray, A. Company, *Chemistry – A European Journal* **2015**, 21, 15029-15038; b) P. Pirovano, A. R. Berry, M. Swart, A. R. McDonald, *Dalton Trans.* **2018**, 47, 246-250.
- [21] a) A. Oda, T. Ohkubo, T. Yumura, H. Kobayashi, Y. Kuroda, *Angew. Chem., Int. Ed.* **2017**, 56, 9715-9718; *Angew. Chem.* **2017**, 129, 9847-9850; b) A. Oda, T. Ohkubo, T. Yumura, H. Kobayashi, Y. Kuroda, *Inorg. Chem.* **2019**, 58, 327-338; c) Y. Shimoyama, T. Kojima, *Inorg. Chem.* **2019**, 58, 9517-9542.
- [22] a) J. Chateaufneuf, J. Luszyk, K. U. Ingold, *J. Am. Chem. Soc.* **1988**, 110, 2886-2893; b) J. Chateaufneuf, J. Luszyk, K. U. Ingold, *J. Am. Chem. Soc.* **1988**, 110, 2877-2885.
- [23] a) F. Thomas, in *Stable Radicals: Fundamentals and Applied Aspects of Odd - Electron Compounds* (Ed.: R. G. Hicks), John Wiley & Sons, Ltd, Chippingham, Wiltshire, UK, **2010**, pp. 281-316; b) C. T. Lyons, T. D. P. Stack, *Coord. Chem. Rev.* **2013**, 257, 528-540.
- [24] a) L. Chiang, R. M. Clarke, K. Herasymchuk, M. Sutherland, K. E. Prosser, Y. Shimazaki, T. Storr, *Eur. J. Inorg. Chem.* **2016**, 2016, 49-55; b) L. Chiang, A. Kochem, O. Jarjayes, T. J. Dunn, H. Vezin, M. Sakaguchi, T. Ogura, M. Orio, Y. Shimazaki, F. Thomas, T. Storr, *Chemistry – A European Journal* **2012**, 18, 14117-14127.
- [25] a) T. Storr, P. Verma, Y. Shimazaki, E. C. Wasinger, T. D. P. Stack, *Chemistry – A European Journal* **2010**, 16, 8980-8983; b) M. Kawai, T. Yamaguchi, S. Masaoka, F. Tani, T. Kohzuma, L. Chiang, T. Storr, K. Mieda, T. Ogura, R. K. Szilagy, Y. Shimazaki, *Inorg. Chem.* **2014**, 53, 10195-10202.
- [26] D. D. Perrin, W. L. F. Armarego, D. R. Perrin, *Purification of Laboratory Chemicals 4th Edition*, 4th ed., Pergamon Press, Elmsford, NY, **1996**.

FULL PAPER

Entry for the Table of Contents



Hydroxylation of alkanes with *m*-CPBA (*m*-chloroperbenzoic acid) catalyzed by Ni^{II}-complexes was investigated. Based on the detailed mechanistic studies, we propose that both (L)Ni^{II}-O• and aryloxy radical species generated by the O–O bond homolysis of a (L)Ni^{II}-*m*-CPBA adduct **a** contribute to the hydrogen atom abstraction process from the substrates in the alkane hydroxylation reaction.